Journal Pre-proofs

Surface Soil Moisture Monitoring with Near-Ground Sensors: Performance Assessment of a Matric Potential-Based Method

D. Serrano, E. Ávila, M. Barrios, A. Darghan, D. Lobo

PII: S0263-2241(20)30079-8
DOI: https://doi.org/10.1016/j.measurement.2020.107542
Reference: MEASUR 107542

To appear in: *Measurement*

Received Date: 29 October 2019
Revised Date: 27 December 2019
Accepted Date: 22 January 2020

SURFACE SOIL MOISTURE MONITORING WITH NEAR-GROUND SENSORS: PERFORMANCE ASSESSMENT OF A MATRIC POTENTIAL-BASED METHOD

Serrano, D.[1]; Ávila, E.[2]; Barrios, M.[3]; Darghan A.[4]; Lobo, D.[5]

[1]Universidad de Córdoba, Facultad de Ciencias Básicas, Colombia. dhelena@correo.unicordoba.edu.co
[2]Universidad del Tolima, Facultad de Ingeniería Agronómica, Colombia. eaavila@ut.edu.co
[3]Universidad del Tolima, Facultad de Ingeniería Forestal, Colombia. mibarrios@ut.edu.co
Universidad Nacional de Colombia. Facultad de Ciencias Agrarias. aqedarghanco@unal.edu.co
[5]Universidad Central de Venezuela, Facultad de Agronomía, Venezuela. lobo.deyanira@gmail.com

Abstract

This study develops an indirect method for the estimation of surface soil moisture (SM) by means of monitoring *in situ* soil water potential. Field work was carried out in ten sampling units selected according to coverage, soil, and topographic factors. Relative humidity and soil temperature were hourly measured to assess the soil-water potential through Kelvin's Law for each sampling unit. Water potential was used as input in the soil moisture retention curve for field conditions to assess SM by fitting the Fredlund-Xing model. To verify the performance of our approach, we measured the surface volumetric SM by the gravimetric method for 2,211 soil samples collected in the same survey period. Results show a non-linear relationship between gravimetric SM and the indirect estimation displaying a determination coefficient of 68.4%. The proposed approach is a suitable exploratory alternative to support continuous SM monitoring studies.

Keywords: monitoring, soil moisture, soil moisture retention curve, soil water potential

1. Introduction

Soil moisture (SM) is a fundamental component of the terrestrial system because it influences water dynamics, the energy and carbon flows between the surface of the earth and the atmosphere, and the distribution of various hydrological mechanisms such as runoff, infiltration and water accumulation in soil processes [1], [2], [3]. However, SM is very variable in space and time; it is heterogeneous due to factors such as precipitation, vegetation, soil texture, topography, and drainage patterns [4]; furthermore, its distribution is influenced by the complex interaction between climatic and environmental effects that dominate SM patterns at the basin scale [5].

Soil moisture is characterized as the combination between the surface SM, which is defined as the water content within the first five centimeters of the soil, and the SM in the root zone defined as the water content below five centimeters of depth [6], [7]. Various methods have been developed to measure SM in the field or under laboratory conditions; these measurements are the main source of information to understand its distribution and variability. Among these methods, the *gravimetry* allows measuring the soil water content, and the *hygrometry* allows measuring the soil-water potential by indirect measurement, each with strengths and limitations [8]. Nonetheless, the estimation of soil moisture has undergone a significant technological development compared to the measurement of water potential in the field as confirmed by [9], [10], and [11], although integrated approaches can overcome the disadvantages of each unique method and produce more robust data [12].

The gravimetric method is a simple, high-level precision method that directly estimates the soil water content (dimensionless mass or volume ratio), obtaining estimates in any moisture range and does not require equipment installation [13], [14], [15], [16]. However, it is time-consuming, laborious, destructive and is often not considered to develop soil moisture networks, but rather to calibrate other moisture sensors or as a reference method for dataset validation obtained with other methods [17], [18].

The soil water potential is a soil property, which allows to indirectly estimate the soil water content by measuring, as is the case, using the relative humidity (RH) and soil temperature (Ts), as variables in the thermodynamic relationship of Kelvin's Law [19]. The estimation of the water content by this technique has a comparative advantage with other methods as it allows inferring the SM in large areas; further, its operation can be automated, it is of low maintenance, soil samples are not destroyed, it does not affect health, and SM can be estimated at any soil depth. On the other hand, it requires high-level calibration equipment and the sensors can be deteriorated over time due to the interaction with the ground [8]. However, new sensors have been designed to facilitate measurements and must be tested to establish their potential for use [20], [9].

[21] evaluated four soil water potential measurement devices, including a cooling hygrometer, a filter paper, a psychrometer, and a relative humidity (RH) sensor. In their study, they established that the RH sensor provided a faster response compared to the other methods and was suitable for water potential measurements in the field and near the soil surface. However, they mentioned that they should have considered that this device may show a systematic error in high RH measurements. Commercially, there are programmable, high fidelity, short time log measurement devices that are an alternative for using under field conditions [22], [23].

To relate the water content and the soil water potential, several empirical models have been developed, which allow elaborating a soil moisture retention curve (SMRC) from the soil moisture saturation state to the residual moisture content due to the potentials in the soil [24], [25], [19], [26]. Among the most common and highly efficient functions used, the Fredlund and Xing (FX) model is highlighted. This model includes three adjustment parameters used to describe the SMRC [27], [28], [25]. However, for water potential measurements in the field, soil hysteresis significantly affects water content estimation, because the same SM magnitude can occur for different potentials or tensions in the soil. This is the reason why [25] suggest an adjustment to the parameters that allow the development of a trajectory or a median retention curve for field condition ($SMRC_f$) depending on the soil texture.

The soil water content estimates in the field, from information on discrete sampling points, requires high density sampling data, which is generally not sufficient due to the variability of the relief, slope, soil type, and vegetation cover that is found in large areas and in mountainous landscapes, in which there are abrupt changes between sampling points [29]. In this sense, the arithmetic average of observations that will be added on a smaller dimension basis may be sensitive to extreme values. Therefore, the incorporation of the lower sensitivity property to the ends (extremes) of the geometric mean can be quite convenient. Thus, the arithmetic mean averaged with the geometric can be more robust to observations that could affect soil moisture measurements [30], [31]. Similarly, although in the statistical properties of the data, the apparent variance and the apparent correlation length are generally different from their true values because of the scale measurement bias; furthermore, also because the apparent variance increases with increasing extent and decreases with increasing support; nonetheless, it does not change with spacing [32].

Accordingly, the aim of this study was to statistically contrast estimates of the water volumetric content of surface soil or volumetric soil moisture (SM) obtained using the gravimetric method (reference method) with SM estimates for soil water potentials obtained by indirect measurement, and the use of the Fredlund-Xing (FX) model that describes the typical soil moisture retention curve developed with adjustment parameters for field conditions ($SMRC_f$). This was carried out in ten sampling units selected according to coverage, soil, and topography factors in the Quindío river basin in Colombia, during seven evaluation periods, between July 2017 and June 2018. This evaluation required continuous monitoring of the SM as a fundamental variable for hydrologic, agronomic, and climate change studies. Although the SM estimation is carried out by different highly recognized field methods, in this case, an alternative method for monitoring SM was used. This method has not been used in Colombia and included the use of the heronian mean and estimates obtained with the FX model that describes the $SMRC_f$ to a series of contrasting sampling units discriminated by cluster analysis in five evaluation strata, and validated with the spatial strata Q statistic. The temporary effect was incorporated initially, but recognizing that in this case, it was not of interest, as verified with the non-parametric longitudinal variance analysis, then, the two humidity measurements were related using a non-linear model.

2. MATERIALS AND METHODS

2.1 Study area

The Quindío River basin is located in the central-western region of the Andean mountain range in Colombia (4°20’55” N, 75°48’04” W and 4°42´57” N, 75°23´ 0” W), with an extension of 688.85 km^2. In the basin, mountainous, foothills, hills and valley landscapes are found with elevations between 1,079 to 4,794 meters above the sea level. Climatically, the region has two rainy seasons or with abundant rains from March to May and from October to December, and the remaining months correspond to dry seasons. According to the records of the climatic stations of La Montaña, La Playa and Centro de la Guadua of Corporación Autónoma Regional del Quindío (CRQ) for 2017, the driest month was July with an average of 45.4 mm, and the rainiest month was November with 310.3 mm. Meanwhile, for the year 2018, the driest month was July with an average of 51.3 mm and the rainiest months were April with 319 mm and October with 317.1 mm, with average temperatures of 17.9 °C in the months of October and November, and 22.1 °C in the months of July and August, with little variation in the average temperature throughout the year.

2.2 Sampling units

The factors that influence the variability of the SM were analyzed to define the sampling units. Coverage, slope, surface curvature, and soil texture were included as variables, as they influence the SM variation, and are used to obtain sampling units representative of the physiographic relief, soil and coverage conditions in the basin as suggested by [33] and [34].

Land cover and land use information were obtained from the map made by Instituto Geográfico Agustín Codazzi (IGAC) [35] at a scale of 1: 25,000 and updated for 2015. The slope and curvature of the surface were acquired from the processing of the 12.5 m Digital Terrain Model (MDT) from the ALOS PALSAR system in Band L, Path 148, Frame 70, and dated February 20, 2011, obtained from the Alaska Satellite Facility (ASF) land data portal. The slope was calculated with the Horn method for rough surfaces, which uses eight neighboring pixels of the cell considered for the calculation [36] and was classified according to the IGAC internal code manual. The curvature was calculated in the direction of the slope with the adjustment coefficients of the eight neighbors near the cell considered; in these, positive values indicate that the surface is concave above the cell, and negative values denote that the surface is convex above the cell; further, values close to zero indicate that the surface is linear [37]. The texture was obtained from the analysis carried out in the soil sample laboratory using the modified Bouyoucos method [38], [14], [15].

A spatial representation with the functionalities of the Geographic Information Systems (GIS) was made to the spatial and attributes information layers, generating an integrated data layer. In this layer, ten candidate sampling units were initially identified, each with an extension of approximately one hectare, with proportional representation of the landscapes and reliefs present in the basin (Figure 1).

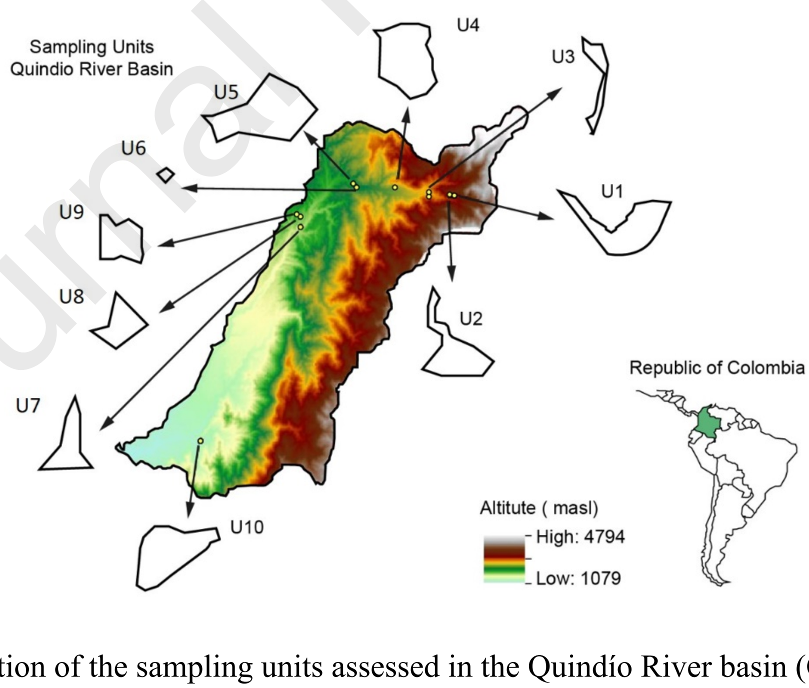

Figure 1. Location of the sampling units assessed in the Quindío River basin (Colombia)

In the mountainous landscape, units U1, U2, U3, U4, U5, and U6, were located between reliefs of rows-cantilever beams and valleys on slopes of 3% and up to 25%. Further, units

U1 and U2 have natural forest cover, herbaceous and shrub vegetation, as well as forest plantations on a convex type surface; the surface soil layer (0-5 cm) has a sandy loam texture (SL). Units U3, U5 and U6 have a pasture cover with clay loam (CL), silt loam (SiL) and clayey (C) soil textures, respectively, as well as convex, concave and linear surfaces, respectively; unit U4 has semi-permanent crops in concave surfaces with a silt loam (SiL) soil texture. The climate in this mountainous area ranges from cold and temperate humid to very humid. The soils in these units have been formed from volcano-sedimentary rocks and thick and medium alluvial deposits, classified as Typic Humudepts, Pachic Hapludands, and Typic Udorthents [35].

Units U7, U8 and U9 are located in foothills and have hilly landscapes; these are located, between reliefs of moderately dissected fans, hills, and ridges, with slopes higher than 25%, with temperate humid and very humid climates, with pasture covers, transitory crops, and permanent shrubs and herbaceous crops. These units have convex and concave surfaces and the soil textures are silt loam (SiL) on U7, and sandy loam (SL) on U8 and U9. The soils of these units have amphibolites, shales, and volcanic ash on torrential volcanic deposits as parental material, and are classified as Typic Humudepts and Typic Hapludands [35].

In the valley landscape with flat flood relief, the U10 unit is located; it is characterized by a slope of 3 to 7%, a convex surface, sandy loam (SL) texture in the superficial soil layer (0-5 cm) covered by vast extensions of *Guadua* spp. (Poaceae) called *guaduales.* The climate is humid temperate, and the soils in this unit come from thick and medium alluvial deposits, classified as Typic Dystrudepts and Typic Endoaquepts [35].

Once the ten units were selected, a regrouping of these units into new similar units was carried out considering the estimated soil moisture contents with the two approaches proposed in the current research. Hence, contrasted moisture content strata were formed once again from which five new sampling units were formed.

2.3 Soil water content (W)

Soil water content was measured in seven evaluation periods or field campaigns in each sampling unit, as follows: from the beginning of the study to 28, 56, 70, 106, 155, 196 and 294 days. In each evaluation period, soil sampling was carried out using the gravimetric method, and the recording of RH and Ts was also performed for indirect estimation of soil water potential, as shown in Figure 2.

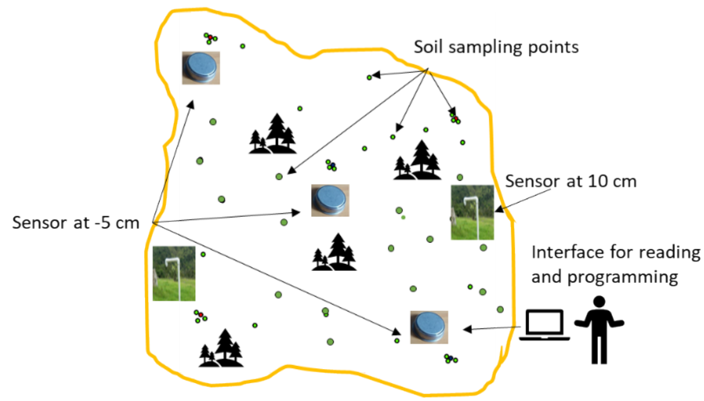

Figure 2. Conceptual model of the field monitoring system for soil sampling and recording of relative humidity and temperature in each candidate sampling unit.

To estimate the volumetric soil moisture, 30 georeferenced random points were established in each sampling unit and at each point, where approximately 20 to 30 g of soil were collected in aluminium capsules, in duplicate and weighed in the field to avoid moisture losses. The SM content was estimated by the gravimetric method, which consisted of drying in the oven at 105 °C for 24 hours the samples collected in the field. These values were subsequently transformed to volumetric humidity values with the soil bulk density [13], [14], [15]. The equation used to estimate the gravimetric humidity (w) is the following (1):

$$w = \frac{M_w}{M_s} \tag{1}$$

Where M_w is the mass of water (g) and M_s is the mass of dry soil (g).

The soil bulk density was obtained from unaltered soil samples collected in rings of 5 cm in diameter by 5 cm in height for analysis by the cylinder method, which relates the total soil mass to the total volume occupied by the sample in the cylinder. Each measurement was made in duplicate [13], [14], [15]. The equation used to estimate the bulk density (ρ) is the following (2):

$$\rho = \frac{M_t}{V_t} \tag{2}$$

Where ρ is the soil bulk density (Mg m^{-3}), M_t is the total soil mass (Mg), and V_t is the total volume occupied by the soil sample (m^3).

Finally, the volumetric humidity θ_o (cm^{-3} cm^{-3}) of equation (3) was estimated using equations (1) and (2), for a total of 2,211 measurements with the following equation:

$$\theta_o = w\frac{\rho}{\rho_w} \tag{3}$$

Where ρ_w represents the water density (Mg m^{-3}).

The calculation of the heronian average of the volumetric moisture labeled θ_H from 2,211 gravimetric humidity values was considered, to group these values into 88 values. These were later confronted with the 88 estimated soil moisture (θ_e) values obtained in each evaluation period per sampling units. The heronian mean (θ_H) has the attribute that it incorporates the arithmetic mean that is the mathematical expectancy of the data, and the geometric mean that has the advantage of not being as sensitive as the arithmetic mean to extreme values, and is relevant when several quantities are multiplied to produce a total; the heronian average is expressed in equation (4).

$$\theta_H = \frac{\frac{1}{n}\sum_{i=1}^{n} x_i + \sqrt[n]{\prod_{i=1}^{n} x_i}}{2} \tag{4}$$

2.4 Volumetric soil water content (θe) by indirect estimation

The relative humidity and temperature were measured with five iButton Hygrochron DS1923 sensors that were installed in each sampling unit, as seen in Figure 2. Three of the sensors were located at a depth of 0-5 cm from the surface into polyurethane capsules and spaced from each other at approximately 50 m. The other two sensors were installed into aerated polyvinyl chloride (PVC) tubes at a height between 10 to 20 cm from the surface and at a distance of around 50 and 70 m from another one. The sensors were programmed for the simultaneous recording of RH (%) and Ts (°C) every 60 minutes. In each evaluation period, the digital download of the measurements and reprogramming of these were performed. Saturation was found in the RH records (> 100%) in several sensors, so adjustments were made to the readings with the methodology proposed by [39]. Therefore, only the RH records of the sensors located above the surface were the ones used in this study as these were more stable and because the RH can be measured in the air phase, in the soil pores or in an area close to the ground [19]. In total, 88 RH values and 88 Ts values were obtained, and each value corresponded with the average of the RH and Ts records at the time of the day and throughout the sampling period in each unit (approximately one hour).

With the averages of RH and Ts, the water potential Ψc (kPa) was calculated as expressed in equation (5) for each evaluation period applying Kelvin's Law, which is a function of the negative relationship between the gas pressure in the soil, and the external pressure of the external gas to the ground [40].

$$\Psi c = -\frac{R\,Ts}{M\left(\frac{1}{\rho_w}\right)} ln(RH) \tag{5}$$

where R is the universal gas constant (8.31432 Joules/mol K); Ts is the absolute soil temperature in degrees °K; M is the molecular weight of water (18.016 kg/kmol); D_w is the density of water (998 kg/m^3), and RH is the relative humidity.

Soil water retention was measured in each sampling unit, for which unaltered soil samples were taken in cylinders of 5 cm in diameter and 2.5 cm in height, at a depth of 0 to 5 cm. The samples were saturated by capillarity, and once a metallic gloss was observed on the surface, they were subjected to air pressures of -10, -30, -100, -500, -1,000 and -1,500 kPa using plates and a pressure chamber (pressure cooker) [41]. For each pressure point, the volumetric soil moisture content (θ) was estimated, and each test was performed in duplicate. Parameters *a, n* and *m* of the FX model expressed by the equation were calculated using equation (6) that describes the SMRC for the drying procedure, where parameter *a* is related to the air entry into the soil pores and determines the turning point of the curve [19]. Parameter *m* is related to the total symmetry of the typical curve and the residual water content; parameter *n* is related to the slope of the curve at the inflection point and the pore size distribution [42]. The above-mentioned calculations were carried out with the Solver program of the Excel spreadsheet and the Generalized Reduced Gradient Nonlinear (GRG) module, including as restrictions, that the parameter values were higher than 0.1, a minimum of 100 iterations in the process, and a convergence value of 0.000001, to avoid very small and negative values.

$$\theta = \theta_r + \frac{(\theta_s - \theta_r)}{[(1 + (\Psi/a)^n)]^m} \tag{6}$$

Where θ is the volumetric moisture (cm^{-3} cm^{-3}) at a certain pressure (Ψ); θ_r is the residual volumetric moisture (cm^{-3} cm^{-3}); θ_s is the volumetric moisture at saturation (cm^{-3} cm^{-3}); and $a, n,$ and m are the adjustment parameters of the models for the curve ($m = 1 - 2/\, n$).

With the methodology proposed by [25], $SMRC_f$ estimation was performed but with the application of a correction factor or lateral adjustment (a_c) to parameter *a,* associated with soil texture, as suggested by the authors; to do so, the particle size distribution was established using the hydrometer method [38] to soil samples from each sampling unit collected from the soil layer at a depth of 0 to 5 cm.

The percentages of sand, silt, and clay were determined, and the textural class was defined for each unit, performing the test on duplicate samples. The lateral adjustment a_c given in equation (7) was made to parameter *a*, and the application of a percentage of 25% for the sampling units U1, U2, U8, U9 and U10 was carried out, as these presented thick or sandy textures; further, 50% adjustment percentage was carried out for sampling units U3, U4, U5, U6, and U7, as they had finer textures; parameters *n* and *m* were left the same to maintain the congruence of the curve.

$$a_c = 10^{Log(a) - \varepsilon} \tag{7}$$

Where, a_c is the adjustment parameter for the $SMRC_f$; a is the adjustment parameter of the SMRC by drying, and ε, is the lateral adjustment percentage.

To estimate the water content (θ_e) based on the soil water potentials measured in the field, the FX model equation was applied as expressed in equation (8), which includes the values calculated in equations (5) and (7).

$$\theta e = \theta_r + \frac{(\theta_s - \theta_r)}{[(1 + (\Psi c/a_c)^n)]^m} \tag{8}$$

Where θ_e is the estimated volumetric moisture (cm^{-3} cm^{-3}) to a certain field water potential (Ψc).

2.5 Statistical analysis

After aggregating different data dimensionality using the heronian average of 2,211 to generate the same data dimension of the FX model (88 measurements), an adjustment was made using cubic splines to the temporal measurements of both moisture modalities, since not all measurements were made exactly the same day due to operational and environmental restrictions. Both measurements were adjusted with the predictions generated from the splines, maintaining seven measurements at 28, 56, 70, 106, 155, 196 and 294 days from the beginning of the study.

Once the moisture measurements were corrected, the effect of time was studied, for which a longitudinal non-parametric analysis of the LDF1 model was used [43]. In this test, the estimated SM values for the candidate sampling unit U8 were discarded by the two estimation modalities, because during the evaluation periods, changes in plant cover and land use in the sampling units were observed in the field, modifying the initial conditions for which this unit was selected. Once the new units were defined, a cluster analysis was performed for both soil moisture measurements adjusted by splines, generating five new units from the nine initial candidate units. The number of clusters was decided based on the discrimination of candidate units within each of the five clusters generated and by the empirical knowledge of the region. Ward's method and the Euclidean distance were used when forming the new units. The generated dendrogram was used to look for the similarity of candidate units within the new units. The validation in the conformation of differentiated groups by moisture or by contrasting moistures used the Q statistic included in the Geodetector library of the R program [44].

Furthermore, a two-dimensional point diagram was made between the two soil moisture modalities generating the convex contours for each of the new sampling units to show the different moisture quantities of each new unit [45].

Finally, the correlation between the heronian averages of the soil moisture with the estimated soil moisture and with the FX model was established, for which a non-linear model was adjusted to predict one modality from the other. The calculations were performed using the programs RStudio and Statgraphics Centurion.

3. Results

Table 1 shows the basic statistics for the heronian average of the SM values obtained by the gravimetric method (θ_H), and the estimated SM values with the FX model (θe) for each initial sampling unit.

Table 1. Mean ($\bar{x}$) and standard deviation (s) for soil moisture (SM) values from the heronian average (θ_H) obtained by gravimetry, and for the estimated values obtained with the FX model (θ_e) per initial sampling unit

Initial sampling units	SM - Heronian average θ_H (cm^{-3} cm^{-3})		SM - Estimated by the FX model θ_e (cm^{-3} cm^{-3})	
	$\bar{x}$	s	$\bar{x}$	s
U1	0.31	0.04	0.35	0.05
U2	0.31	0.07	0.33	0.04
U3	0.54	0.08	0.57	0.06
U4	0.50	0.10	0.52	0.02
U5	0.53	0.08	0.50	0.08
U6	0.51	0.11	0.46	0.06
U7	0.45	0.08	0.47	0.06
U9	0.44	0.05	0.43	0.04
U10	0.41	0.08	0.42	0.10

The graphs of the cubic splines applied to the values of the heronian average (θ_H) as well as to the SM estimates by the FX model (θ_e) of the initial sampling units are observed in Figure 3. This allowed interpolating the SM for the evaluation periods at 28, 56, 70, 106, 155, 196, and 294 days from the beginning of the study.

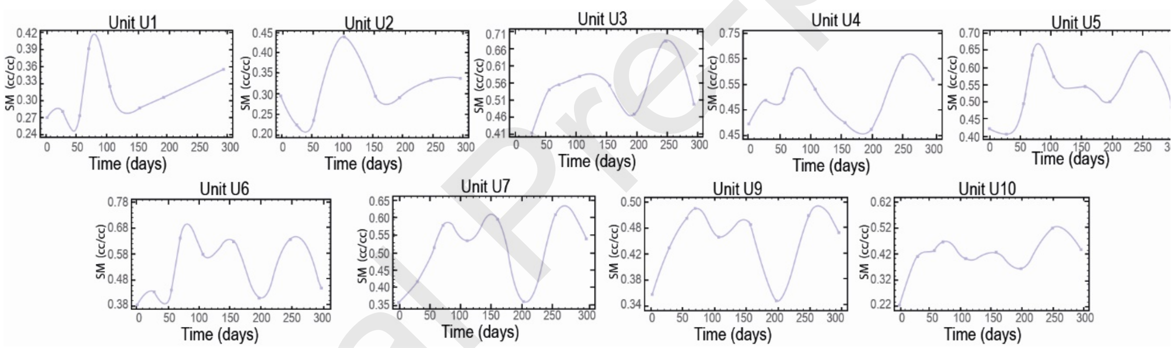

(a)

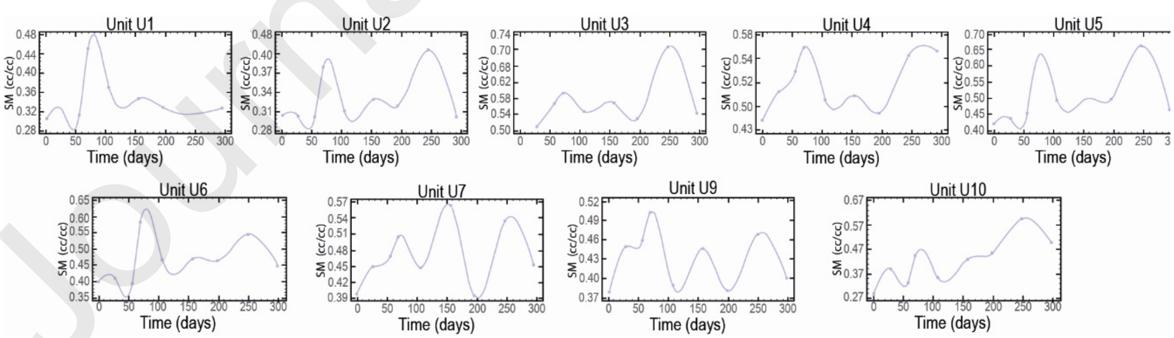

(b)

Figure 3. Interpolation graphs by cubic splines of the heronian average (a), and the FX model estimates (b) per sampling unit.

The effect relative to the time between the heronian mean values (θ_H) and the estimated values with the FX model (θ_e) performed with the analysis of variance of repeated measures (longitudinal) of the non-parametric approach using the Hotelling test in an LD_f1 design, showed for a statistic of 5.38, a *p*-value of 0.098 for the θ_H values, and for the 4.82 statistic, a *p*-value of 0.112 for the θ_e values, each with 6 degrees of freedom.

Figure 4 is a comparative graph of the time series that shows similar variances in four evaluation periods, corresponding to 56 (October/2017), 70 (November/2017), 156 (February/2018) and 294 (June/2018) days for the two SM estimation methods. A slight increase in the variance in the evaluation periods in days 28 (September/2017) and 196 (March/2018), and a smaller variance in day 106 (December/2017) of the estimated values (θ_e) compared to the heronian averages (θ_H) was observed. However, statistically, there is no time-related effect for the heronian averages (θ_H) or the estimated values (θ_e).

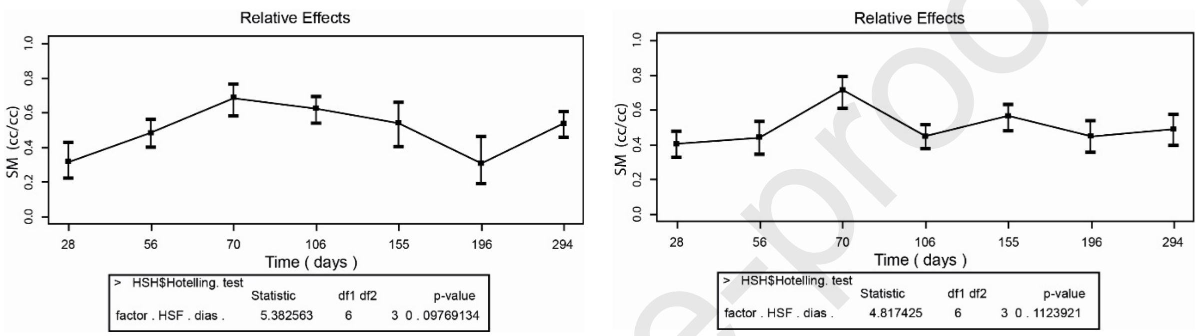

a) b)

Figure 4. Effect relative to the evaluation time with the heronian mean (a) and the estimated soil moisture (b).

With the averages adjusted to the evaluation periods, the cluster analysis allowed grouping nine initial sampling units into five strata of high similarity in soil moisture values; where, cluster C1 was comprised by sampling units U1 and U2 in equal representation percentage of 50%; cluster C2 was mainly composed of units U7 and U10, each with a representation of 40.1%; in the C3 cluster, units U4 and U5 were incorporated in higher representation, each with a percentage of 29.99%; the C4 cluster was mainly composed of the units U6 with a percentage of 19.97%, and of the U9 unit with 29.99%; and finally, cluster 5 incorporated the U3 unit with a representation of 40.01% (see the dendrogram in Figure 5).

.

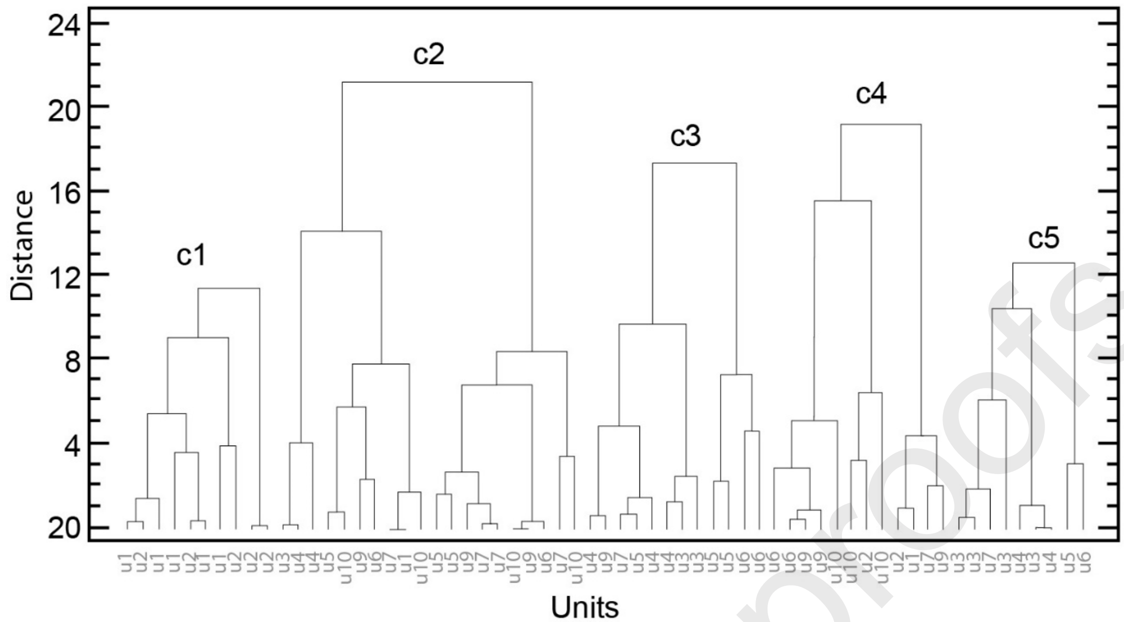

Figure 5. Dendrogram formed by the sampling units in the cluster analysis (Ward's method and distance Euclidean)

The representation of the dendrogram (Figure 5) allows observing that cluster c1 represented 15.87% of the set of conglomerates, and the sampling units that formed this cluster have a similar landscape, relief, surface curvature, slope, and soil type conditions; nonetheless, differences in plant cover were observed. Cluster c2, represented 31.75% of the set of conglomerates, and the units that formed this cluster are different in landscape conditions, relief, soil texture, and vegetation cover; however, they are coincident in topography with slopes of less than 12%. Cluster c3 accounted for 19.05% of the set of conglomerates, and the units that comprised this cluster are located in a similar landscape, relief and soil type, although they show a difference in slope, surface curvature, and vegetation cover. Cluster c4 represents 19.05% of the set of conglomerates, and the units included, have comparative differences between each other in all soil and vegetation cover conditions; however, these units showed a strong change dynamic during the study period in plant cover, as the soil surface in the field was exposed without vegetation, possibly causing this behavior. Finally, cluster c5 represented 14.29% of the cluster of conglomerates and was formed with only one sampling unit, which makes it particularly homogeneous in soil conditions and vegetation cover. The cluster conformation validation with the Q test showed a *p*-value <0.00001 with a statistic of 0.8134, proving that there is a clear definition of the five SM clusters.

The two-dimensional point diagram and the convex contour function between the adjusted heronian average (θ_H) with the estimated moisture (θ_e) by the FX model, defined cluster 1 with SM values between 0.22 cm^3 cm^{-3} and 0.35 cm^3 cm^{-3}; cluster 2, with SM values between 0.36 cm^3 cm^{-3} and 0.51 cm^3 cm^{-3}; cluster 3, with SM values between 0.46 cm^3 cm^{-3} and 0.63 cm^3 cm^{-3}; cluster 4, with SM values between 0.31 cm^3 cm^{-3} and 0.45 cm^3 cm^{-3}; and cluster 5, with SM values between 0.53 cm^3 cm^{-3} and 0.64 cm^3 cm^{-3}, as shown in Figure 6.

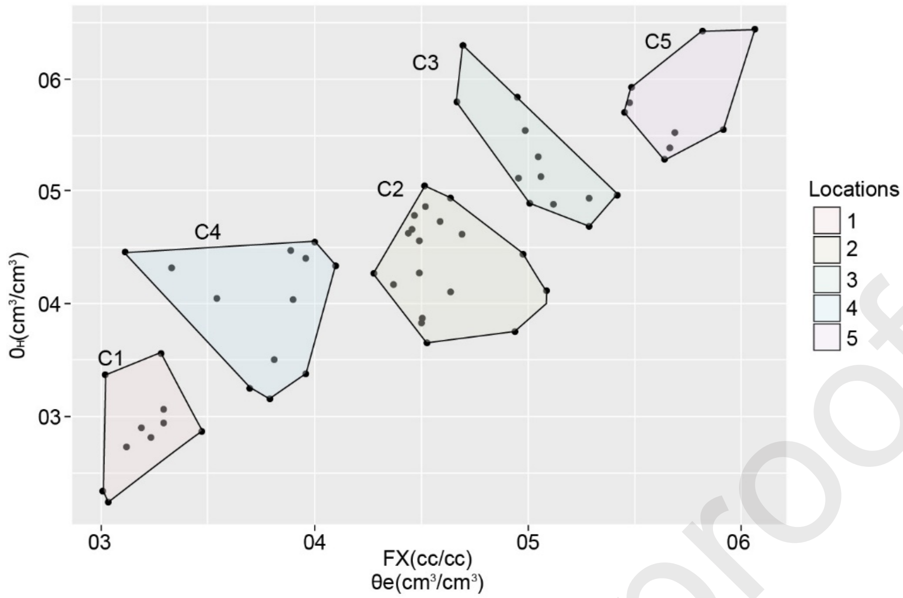

Figure 6. Convex contours of soil moisture values formed between the heronian average (adjusted by splines) of gravimetric moisture and the moisture estimated with the FX model.

Lastly, the non-linear model with the greatest adjustment between the heronian averages and the moisture estimated by the FX model presented a coefficient of determination of 68.4% and an adjusted coefficient of determination of 67.9%; and although the interest in this study did not include the comparison between models, as the uselessness of this measure is recognized in the context of non-linear models [46] the proposed model can be adopted to predict the heronian average of the soil volumetric moisture for SM estimates using the FX model with field parameters (Figure 7).

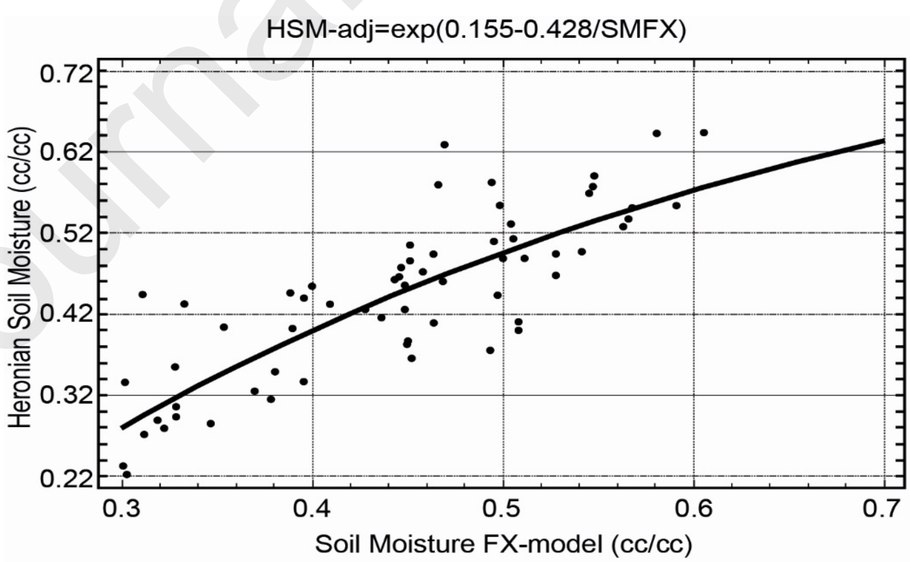

Figure 7. Adjusted nonlinear model of soil surface moisture between the heronian average and the FX model estimates.

4. Discussion

This study compared the SM estimates obtained by indirect measurement of the soil water potential and the use of the FX model adjusted with field parameters, with estimates obtained using the gravimetric method that is highly recognized for its accuracy and use as a reference method in sampling units for soil conditions and vegetation cover in the Quindío river basin. One of the most important aspects of this evaluation was to estimate the heronian average for volumetric moisture estimates per evaluation period, as an alternative to statistically compare and evaluate the two soil-surface moisture estimation measurements in the initial sampling units. For this, grouping the number of measurements obtained by the gravimetric method and relate them to a lower number of estimates obtained with the FX model was required, softening part of the variability when the averages are considered; furthermore, the increase in support increases the robustness of the estimates in the analysis as indicated by [32].

When evaluating the quality of the estimates by the two methodologies used, the results showed that there was no effect relative to the time, i.e., the variations were similar in behavior during the evaluation period that included the rainy and the dry seasons, which evidenced that presumably, the results might be due to other heterogeneous factors. Among these, the curvature of the surface that favors the accumulation of moisture or influences water loss is highlighted. These results coincide with the study carried out by [33], who reported that the moisture percentages of the sites they evaluated maintained the same condition during the rainy and the dry seasons, that is, those with the highest moisture in the dry season were also those with the highest moisture in the rainy season, a condition that was observed mainly in the behavior of the moisture estimates by the two methodologies in cluster c5.

As mentioned by [47] slope and soil texture are the variables with the highest incidence in SM and influence water flows, showing runoff losses on steep slopes, a condition that occurs in clusters c1, c3, c4 and c5 (slopes greater than 30%). This contrasts with the smoother slopes and flat or convex surfaces in which the flow through runoff slows down and can increase the amount of water in the soil by accumulation, as can be observed in cluster c2. In addition, the variability of the SM surface at the basin scale may be influenced by factors such as precipitation, variations of incoming solar radiation to the ground and the wind that can influence the evapotranspiration rate of the soil by increasing or decreasing SM; further, as proposed by [48], the variability of the surface SM may be higher after a rainfall period due to the effects of soil heterogeneity, as presumably occurs in this basin.

Similarly, land use and changes in vegetation cover significantly influence the variability of SM, as observed in the field in cluster c4 for an evaluation period, because these changes are associated with infiltration and runoff rates; nevertheless, a more drastic effect can be evidenced in the growing season of the crop as indicated by [49].

The researchers agree that the estimation of soil moisture by sampling soil in the field is complex in terms of time and resources, and demands a large number of samples due to the spatial variability of the soil [50], [11], [8], [10]. However, the results showed a clear statistical relationship between the heronian average (which initially had a higher number of measurements) with the measurements of the water potential in the field and the FX model estimates (with the least number of measurements) even in contrasting moisture scenarios for the defined sampling units, without having to build a nested model for each unit. In this way, the performance of the indirect SM estimation was consistent and is an adoptable alternative that can support continuous SM monitoring studies.

Conclusions

The results of our study show that soil surface moisture estimates obtained by indirect estimation of the soil water potential in the field related in the Fredlund-Xing model with adjustment parameters for soil texture show a high statistical relationship with the estimates obtained through the gravimetric method, even in contrasting moisture values. Therefore, this method can be considered as an alternative for monitoring soil moisture without having a scale effect problem, since the same support and the same amplitude were maintained in the triplet that comprises the spatial scale.

Acknowledgment

This research was funded by Universidad del Tolima [Project 550116]. The authors wish to thank Corporación Autónoma Regional del Quindío (CRQ) for financing and giving the logistical support for this study, and also to Universidad del Tolima, particularly to the Soil Physics Laboratory of the Faculty of Agricultural Engineering.

Bibliographic references

[1] Peng, J., Loew, A. (2017). Recent advances in soil moisture estimation from remote sensing. *Water*, *9*(7), 530; https://doi.org/10.3390/w9070530.

[2] Tuttle, S. E., Salvucci, G. D. (2014). A new approach for validating satellite estimates of soil moisture using large-scale precipitation: Comparing AMSR-E products. *Remote Sensing of Environment*, *142*, 207-222. doi.org/10.1016/j.rse.2013.12.002.

[3] Kerr, Y. H., Wigneron, J. P., Al Bitar, A., Mialon, A., Srivastava, P. K. (2016). Soil Moisture from Space: Techniques and Limitations. In: *Satellite Soil Moisture Retrieval*. *Techniques and Applications* (pp. 3-27). Elsevier. doi.org/10.1016/B978-0-12-803388-3.00001-2.

[4] Korres, W., Reichenau, T.G., Schneider, K. (2013). Patterns and scaling properties of surface soil moisture in an agricultural landscape: An ecohydrological modeling study. *Journal of Hydrology*, 498, 89–102. doi.org/10.1016/j.jhydrol.2013.05.050.

[5] Crow, W. T., A. A. Berg, M. H. Cosh, A. Loew, B. P. Mohanty, R. Panciera, P. de Rosnay, Ryu, D., Walker, J. (2012). Upscaling sparse ground-based soil moisture observations for the validation of coarse-resolution satellite soil moisture products, *Rev. Geophys.*, 50(2), RG2002. doi.org/10.1029/2011RG000372.

[6] Hillel, D. (1998). *Environmental Soil Physics*, Academic Press, San Diego, CA.

[7] Seneviratne, S. I., T. Corti, E. L. Davin, M. Hirschi, E. B. Jaeger, I. Lehner, B. Orlowsky, A. J. Teuling (2010). Investigating soil moisture-climate interactions in a changing climate: A review, *Earth Sci. Rev*., 99, 125–161.

[8] Petropoulos, G. P., Ireland, G., Barrett, B. (2015). Surface soil moisture retrievals from remote sensing: Current status, products & future trends. *Physics and Chemistry of the Earth, Parts A/B/C*, *83*, 36-56. doi.org/10.1016/j.pce.2015.02.009.

[9] Whalley, W. R., Ober, E. S., Jenkins, M. (2013). Measurement of the matric potential of soil water in the rhizosphere. *Journal of Experimental Botany*, *64*(13), 3951-3963. doi.org/10.1093/jxb/ert044.

[10] Romano, N. (2014). Soil moisture at local scale: Measurements and simulations. *Journal of Hydrology*, *516*, 6-20. doi.org/10.1016/j.jhydrol.2014.01.026.

[11] Durner, W., Or, D. (2006). Soil water potential measurement. *Encyclopedia of hydrological sciences*. *Part 6.* doi.org/10.1002/0470848944.hsa077a.

[12] Brocca, L.; Hasenauer, S.; Lacava, T.; Melone, F.; Moramarco, T.; Wagner, W.; Dorigo, W.; Matgen, P.; Martinez-Fernandez, J.; Llorens, P.; Latron, J.; Martin, C.; & Bittelli, M. (2011). *Soil moisture estimation*

*through ASCAT and AMSR-E sensors: An intercomparison and validation study across Europe. Remote Sens. Environ. 2011, 115, 3390–34*08. doi.org/10.1016/j.rse.2011.08.003.

[13] Forsythe, W. (1975). *Física de suelos: Manual de Laboratorio* (Vol. 25). Instituto Interamericano de Cooperación para la Agricultura (IICA). San José, Costa Rica.

[14] Pla, I. (1983). Metodología para la caracterización física con fines de diagnóstico de problemas de manejo y conservación de suelos en condiciones tropicales. Revista de la Facultad de Agronomía. Alcance 32. Universidad Central de Venezuela (Venezuela). ISSN: 0041-8225.

[15] Gabriels, D., Lobo, D. (2006). Métodos para determinar granulometría y densidad aparente del suelo. *Venesuelos*, *14*(1), 37-48.

[16] Florentino, A. (2006). Métodos para medir el contenido de agua en el suelo. *Venesuelos*, *14*(1), 48-70.

[17] Ochsner, T. E., Cosh, M. H., Cuenca, R. H., Dorigo, W. A., Draper, C. S., Hagimoto, Y., Kerr, Y.H., Njoku, E.E, Zreda, M. Larson, K.M. (2013). State of the art in large-scale soil moisture monitoring. *Soil Science Society of America Journal*, *77*(6), 1888-1919. doi:10.2136/sssaj2013.03.0093.

[18] Zhuo, L., Han, D. (2016). The relevance of soil moisture by remote sensing and hydrological modelling. *Procedia Engineering*, *154*, 1368-1375. doi.org/10.1016/j.proeng.2016.07.499.

[19] Meza, V. (2012). Suelos parcialmente saturados, de la investigación a la cátedra universitaria. *Boletín de Ciencias de la Tierra*, (31), 23-38. Disponible en: http://www.redalyc.org/articulo.oa?id=169524098003.

[20] Bakker, G., van der Ploeg, M. J., de Rooij, G. H., Hoogendam, C. W., Gooren, H., Huiskes, C., koopal, L., Kruidhof, H. (2007). New polymer tensiometers: Measuring matric pressures down to the wilting point. *Vadose Zone Journal*, *6*(1), 196-202. doi:10.2136/vzj2006.0110.

[21] Agus, S. S., Schanz, T. (2005). Comparison of four methods for measuring total suction. *Vadose Zone Journal*, *4*(4), 1087-1095. doi: 10.2136/vzj2004.0133.

[22] Shin, M., Patton, R., Mahar, T., Ireland, A., Swan, P., Chow, C. M. (2017). Calibration and validation processes for relative humidity measurement by a Hygrochron iButton. *Physiology & Behavior*, *179*, 208-212. doi.org/10.1016/j.physbeh.2017.06.019.

[23] Chelli, S., Canullo, R., Campetella, G., Schmitt, A. O., Bartha, S., Cervellini, M., Wellstein, C. (2016). The response of sub-Mediterranean grasslands to rainfall variation is influenced by early season precipitation. *Applied Vegetation Science*, *19*(4), 611-619. doi.org/10.1111/avsc.12247.

[24] Fredlund, D. G., Xing, A. (1994). Equations for the soil-water characteristic curve. *Canadian Geotechnical Journal*, *31*(4), 521-532. doi.org/10.1139/cgj-2018-0189.

[25] Fredlund, D. G., Sheng, D., Zhao, J. (2011). Estimation of soil suction from the soil-water characteristic curve. *Canadian Geotechnical Journal*, *48*(2), 186-198. doi.org/10.1139/T10-060.

[26] Hincapié Gómez, E., Tobón Marín, C. (2012). Dinámica del agua en andisoles bajo condiciones de ladera. *Revista Facultad Nacional de Agronomía Medellín, 65(2), 6765 - 6777. Disponible en: http://www.redalyc.org/articulo.oa?id=179925831019.*

[27] Alfaro, M. (2008). Geotecnia en suelos no saturados. Rev. Acad. Colomb. Cienc. 32(125), 471-481.

[28] Ochoa, V. E. M., Patiño, F. H. (2012). Influencia de la succión matricial en el cambio de volumen de un suelo proveniente de un depósito aluvial del Valle de Aburrá. *Revista Facultad de Ingeniería Universidad de Antioquia*, (64), 104-114. Disponible en: http://www.redalyc.org/articulo.oa?id=43025083009.

[29] Goovaerts, P. (1999). Geostatistics in soil science: state-of-the-art and perspectives. *Geoderma*, *89*(1-2), 1-45. doi.org/10.1016/S0016-7061(98)00078-0.

[30] Sýkora, S. (2009). Mathematical means and averages: Generalized Heronian means. *Stan's Library: Castano Primo, Italy*. doi: 10.3247/SL3Math09.002.

[31] Wilson, D. J., Western, A. W., Grayson, R. B. (2005). A terrain and data-based method for generating the spatial distribution of soil moisture. *Advances in Water Resources*, *28*(1), 43-54. doi.org/10.1016/j.advwatres.2004.09.007.

[32] Western, A. W., Blöschl, G. (1999). On the spatial scaling of soil moisture. *Journal of Hydrology*, *217*(3-4), 203-224. doi.org/10.1016/S0022-1694(98)00232-7.

[33] Martínez-González, F., Sosa-Pérez, F., Ortiz-Medel, J. (2010). Comportamiento de la humedad del suelo con diferente cobertura vegetal en la Cuenca La Esperanza. *Tecnología y Ciencias del Agua*, *1*(4), 89-103. *versión On-line* ISSN 2007-2422.

[34] Yee, M. S., Walker, J. P., Monerris, A., Rüdiger, C., Jackson, T. J. (2016). On the identification of representative in situ soil moisture monitoring stations for the validation of SMAP soil moisture products in Australia. *Journal of Hydrology*, *537*, 367-381. doi.org/10.1016/j.jhydrol.2016.03.060.

[35] IGAC - Instituto Geográfico Agustín Codazzi. (2013). Estudio semidetallado de Suelos Departamento del Quindío Escala 1:25000. Informe técnico.

[36] Horn, B. K. (1981). Hill shading and the reflectance map. *Proceedings of the IEEE*, *69*(1), 14-47. doi: 10.1109/PROC.1981.11918.

[37] Zevenbergen, L. W., Thorne, C. R. (1987). Quantitative analysis of land surface topography. *Earth surface processes and landforms*, *12*(1), 47-56. doi.org/10.1002/esp.3290120107.

[38] Day, P. R. (1965). *Particle fractionation and particle-size analysis*. In C.A. Black, ed. Methods of soil analysis, Part 1. Agronomy No. 9. American Society of Agronomy, Madison, WI.

[39] Ashcroft, M. B., Gollan, J. R. (2013). Moisture, thermal inertia, and the spatial distributions of near-surface soil and air temperatures: understanding factors that promote microrefugia. *Agricultural and Forest Meteorology*, *176*, 77-89. doi.org/10.1016/j.agrformet.2013.03.008.

[40] Fredlund, D. G., Rahardjo, H., Rahardjo, H. (1993). *Soil mechanics for unsaturated soils*. John Wiley & Sons. Inc., New York.

[41] Pla, I. (2010). Medición y evaluación de propiedades físicas de los suelos: dificultades y errores más frecuentes. *Propiedades Mecánicas. Suelos Ecuatoriales*, *40*(2), 75-93.

[42] Lu, N., Likos, W. J. (2004). *Unsaturated soil mechanics*. Wiley.

[43] Noguchi, K., Gel, Y. R., Brunner, E., Konietschke, F. (2012). nparLD: and R software package for the nonparametric analysis of longitudinal data in factorial experiments. *Journal of Statistical Software*, *50*(12). http://resolver.sub.uni-goettingen.de/purl?gs-1/9492. doi: 10.18637/jss.v050.i12.

[44] Wang, J. F., Zhang, T. L., Fu, B. J. (2016). A measure of spatial stratified heterogeneity. *Ecological Indicators*, *67*, 250-256. doi.org/10.1016/j.ecolind.2016.02.052.

[45] Van Kreveld, M., Schwarzkopf, O., de Berg, M., Overmars, M. (2000). *Computational geometry algorithms and applications*. Springer.

[46] Spiess, A. N., Neumeyer, N. (2010). An evaluation of R^2 as an inadequate measure for nonlinear models in pharmacological and biochemical research: a Monte Carlo approach. *BMC pharmacology*, *10*(1), 6. https:// doi: 10.1186/1471-2210-10-6.

[47] Harold, W., Hocker Jr, C. (1984). *Introducción a la Biología Forestal. Primera edición en español. México, D.F.: A.G.T. Editor, S.A*

[48] Reynolds, S. G. (1970). The gravimetric method of soil moisture determination Part I. A study of equipment, and methodological problems. *Journal of Hydrology*, *11*(3), 258-273. doi.org/10.1016/0022-1694(70)90066-1.

[49] Zhao, Y., Peth, S., Reszkowska, A., Gan, L., Krümmelbein, J., Peng, X., Horn, R. (2011). Response of soil moisture and temperature to grazing intensity in a Leymus chinensis steppe, Inner Mongolia. *Plant and soil*, *340*(1-2), 89-102. doi.org/10.1007/s11104-010-0460-9.

[50] Klute, A. (1986). Water retention: Laboratory methods, Methods of Soil Analysis, Part I, A. Klute, 635–660. *Am. Soc. Agron., Madison, Wisc*.

Highlights:

- An indirect estimation of surface soil moisture (SM) was developed
- The method assesses in situ water potential and applies a fitted Fredlund-Xing model.
- A high statistical relationship with gravimetric SM measurements was obtained

Credit Author Statement

Contribution by author:

Serrano, D.: Data collecting, data processing, analysis
Ávila, E.: Sampling design, field and lab work coordination
Barrios, M.: Formal analysis, Discussion, Funding acquisition
Darghan A.: Statistical analysis, data processing
Lobo, D.: Conceptualization, Methodological approach